Thin Solid Films 612 (2016) 310–316

Contents lists available at ScienceDirect

Thin Solid Films

journal homepage: www.elsevier.com/locate/tsf

Grain size and lattice parameter's influence on band gap of SnS thin nano-crystalline films

Yashika Gupta [a,b], P. Arun [a,*], A.A. Naudi [c], M.V. Walz [c], E.A. Albanesi [c,d]

[a] Department of Electronics, S.G.T.B. Khalsa College, University of Delhi, Delhi 110007, India
[b] Department of Electronic Science, University of Delhi-South Campus, New Delhi 110021, India
[c] Facultad de Ingeniería, Universidad Nacional de Entre Ríos, 3101 Oro Verde (ER), Argentina
[d] Instituto de Física del Litoral (CONICET-UNL), Guemes 3450, 3000 Santa Fe, Argentina

ARTICLE INFO

Article history:
Received 4 January 2016
Received in revised form 23 May 2016
Accepted 31 May 2016
Available online 6 June 2016

Keywords:
Chalcogenides
Thin films
Vapor deposition
X-ray diffraction
Electronic structure

ABSTRACT

Tin sulphide nano-crystalline thin films were fabricated on glass and Indium Tin Oxide (ITO) substrates by thermal evaporation method. The crystal structure orientation of the films was found to be dependent on the substrate. Residual stress existed in the films due to these orientations. This stress led to variation in lattice parameter. The nano-crystalline grain size was also found to vary with film thickness. A plot of band-gap with grain size or with lattice parameter showed the existence of a family of curves. This implied that band-gap of SnS films in the preview of the present study depends on two parameters, lattice parameter and grain size. The band-gap relation with grain size is well known in the nano regime. Experimental data fitted well with this relation for the given lattice constants. The manuscript uses theoretical structure calculations for different lattice constants and shows that the experimental data follows the trend. Thus, confirming that the band gap has a two variable dependency.

1. Introduction

The photovoltaic industry has been growing rapidly over the recent years due to the increasing demand for low cost and yet high efficiency solar cells. Tin sulphide (SnS), a IV-VI group semiconductor, having an orthorhombic double layered structure with weak Van der Waals bonds between the layers, is considered a potential candidate due to its properties like high absorption coefficient (~10^4 cm^{-1}) and band gap (of the order of ~1.1–1.6 eV) [1,2]. SnS films are amphoteric in nature, i.e., they can exist either as 'n'-type or 'p'-type, depending on the fabrication conditions [3,4]. SnS properties are also anisotropic [5–7], which, along with its amphoterism demand an extensive investigation.

We have noticed that the orientation of the SnS films depends on the substrate it is grown on. This in turn influences the lattice parameters. In this study we have detailed the difference in properties of SnS films grown on glass and ITO substrates. Glass and ITO were selected as substrates because of their cost and easy availability. Also, ITO is widely used in solar cell applications as an electrode. There are few reports in literature where Molybdenum coated substrates have also been used in solar cells to obtained oriented films [8].

The grain size of the films grown on glass and ITO substrates also showed thickness dependence. This encouraged us to study the properties of SnS thin films, such as band gap, as a function of grain size and lattice parameters. We are in a position to experimentally comment on the effective mass of the charge carriers. Finally, we have corroborated our experimental results with the theoretical calculations made. Though the grain size of SnS films are far smaller than what would be useful in photo-voltaics, our study characterizes SnS thin films and shows how lattice parameter and grain size effect its properties. This indicates how we can control and tune the properties according to the required application.

2. Experimental

Thin SnS films of varying thicknesses were fabricated by thermal evaporation of SnS pellets on optically flat glass and ITO substrates (150 nm thick layer of Indium tin oxide grown on glass substrate) maintained at room temperature, using a Hind High Vac (12A4D) thermal evaporation coating unit at vacuum better than 4×10^{-5} Torr. The deposition rate was maintained at 2.7 Å/s for all fabrications to ensure n-type conductivity [9]. P-type SnS films are obtained with the same starting SnS material when it is evaporated on glass substrates maintained at temperatures greater than 280 °C. Results from five different thicknesses (270–900 nm) grown on glass and ITO substrates are reported in this study. The thicknesses used for glass substrates were 270, 480, 600, 650 and 900 nm, while those on ITO substrates were 330, 430, 500, 610 and 800 nm thick. The starting material was 99.99% pure SnS

* Corresponding author.
E-mail address: arunp92@physics.du.ac.in (P. Arun).

http://dx.doi.org/10.1016/j.tsf.2016.05.056
0040-6090/

powder provided by Himedia (Mumbai). The thickness of the films was measured using Dektak surface profiler (150). The structural analysis of the samples was done using X-ray diffractometer (Bruker D8 X-ray diffractometer) operating at 40 kV, 40 mA with CuKa radiation (λ = 1.5406 Å) and Transmission Electron Microscopy (Technai T30U Twin). The optical absorption and transmission spectra of the films were recorded using a UV–Vis Double Beam Spectrophotometer (Systronics 2202) over the range of 300–1000 nm. The Hot-probe measurements confirmed films were of n-type. The chemical composition of the starting material and films were confirmed by X-ray photo-electron spectroscopy (XPS), energy-dispersive X-ray spectroscopy (EDS) and Raman analysis and have been reported earlier [10].

3. Results and discussion

3.1. The structural and morphological analysis

In this study, we have compared n-type SnS films grown on glass and ITO substrates of different thicknesses. The X-ray diffraction (XRD) profile for two comparable thicknesses is shown in Fig. 1. All the films grown on glass substrates showed the (040), (131) and (151) prominent peaks. However, films fabricated on ITO substrates showed ITO peaks whose contribution decreased with increasing thickness. Both diffraction patterns matched well with the orthorhombic structure reported in ASTM card 83-1758, which reported the lattice parameters as a = 4.148 Å, b = 11.48 Å and c = 4.177 Å and *Pnma* space group [11]. While the diffraction peaks corresponding to the (040), (131) and (151) planes were prominent for films grown on glass substrates, the films on ITO substrates showed the peaks corresponding to the (040), (041), (200) and (151) planes.

To investigate further, we have studied the samples using High Resolution Transmission Electron Microscope (HRTEM). Films were scrapped off the substrate using surgical blade and dusted/transferred to copper grids. The HRTEM images of SnS film on glass and ITO substrates are shown in Fig. 2. The layered structure of the films is evident from the parallel lines seen. The inter-planar distances can be directly measured from these images. The inter-planar distance can also be calculated from XRD data using the formula [12].

$$\frac{1}{d^2}=\frac{h^2}{a^2}+\frac{k^2}{b^2}+\frac{l^2}{c^2} \tag{1}$$

where a, b, c are the lattice parameters and h, k, l are the Miller indices given in the ASTM card. The inter-planar distances evaluated from HRTEM micro-graphs of samples grown on glass were found to be around 0.285 nm. Considering that b/4 ≈ 0.285nm, this would imply that the lines seen in the micrograph are SnS layers arranged in the 'ac' plane with 'b' axis parallel to the substrate, or we may say our films have preferred orientation with the (040) planes perpendicular to the substrate. This orientation promises to be mechanically stable [13]. However, inter-planar distances measured from the micrographs of samples grown on ITO substrates are ≈0.31nm. This is due to the 'ac' planes making an angle of ≈67° caused by the 'b' axis, making an angle of ≈23° with respect to the substrate (see Fig. 3).

Other than exhibiting polycrystallinity, fabricated films also exist in a state of stress, as is evident from the compressions or elongations experienced by the lattice. The lattice is said to be in a state of stress, also referred as "residual stress". Residual stress are remnant, unbalanced forces existing in the lattice due to the rapid condensation of material during film fabrication, or due to curvature on the substrate and/or due to the film-substrate interface, etc. Residual strain can be evaluated from the displacement of the X-ray diffraction peaks from which lattice parameters are then evaluated. The lattice strain is given as [14].

$$\delta=\frac{l_{OBS}-l_{ASTM}}{l_{ASTM}} \tag{2}$$

where 'l' is the lattice parameter of the observed (subscript 'OBS') and single crystal (subscript 'ASTM') sample. Using the values of the elastic constants, the stress can be calculated using the determined strain data. We have calculated the lattice parameters for all our samples and shall comment on their significance subsequently.

To investigate the variation of grain size with substrate and film thickness, we have calculated the average grain size of the films. The calculations were made using the Full Width at Half Maxima (FWHM) of the XRD peaks in the Scherrers formula [12].

$$r=\frac{0.9\lambda}{\beta\cos\theta} \tag{3}$$

where 'r' is the grain size, β is the FWHM, θ and λ have their usual meaning. The grain sizes were found to vary from 11 to 18 nm, depending on the film thickness in both substrates. However, it is clear from Fig. 4 that, for comparable film thickness, we get larger grains of SnS on ITO substrates. Devika et al. [15] have argued that SnS nucleation is easier on ITO than on glass because of its crystalline nature. The error bars in the graphs were calculated by taking the step size of the instruments into account and repeating the calculations using the step size as the least count of the instrument. The variation in grain size between films grown on ITO and glass is well above the error bars.

We have observed that SnS films on glass substrates have the same values for 'b' and 'c' as in single crystals. However a tensile stress exists along the 'a' direction (i.e. $a_{OBS} > a_{ASTM}$). In contrast to this, samples on ITO show a compression along the 'c' direction which, within experimental limits, is constant for all film thicknesses. The lattice parameter 'b' remains equal to that of single crystal (see Table 1A). Similar to the case of films on glass, here also a tensile stress exists along the 'a' axis. To summarize, SnS films grown on ITO have an exaggerated tensile force acting along the 'a' direction and compressive forces acting along the 'c' direction resulting from the 'b' axis not being parallel to the ITO substrate (see Table 1B). This, gives us an opportunity to study the properties of SnS films and look into variation caused by grain size, lattice parameter and orientation.

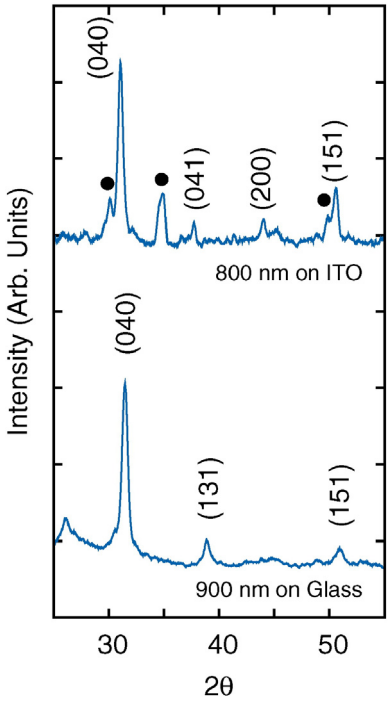

Fig. 1. X-ray diffraction pattern of SnS films of comparable thicknesses grown on glass and ITO substrates. Filled circles indicate peaks of ITO substrate.

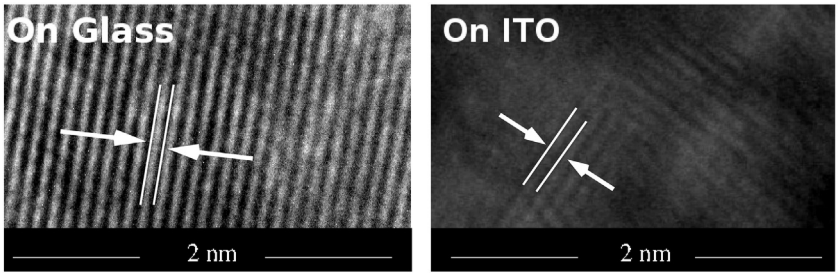

Fig. 2. Transmission electron microscope images compare the layered structure of SnS films on glass and ITO substrates. Parallel lines shown between arrows mark the distance between two planes.

3.2. Optical analysis

The optical properties of a material are represented by its band gap and refractive index. Both information are evaluated from the UV–visible absorption-transmission spectra. The absorption coefficient ('α') is calculated, after which, the band gap of the films are obtained by extrapolating the linear part of $(\alpha h\nu)^2$ vs $h\nu$ plot to the 'X'-axis, using the standard Tauc method [16]. The variation of the direct band gap with grain size of SnS films, grown on ITO and glass substrates are shown in Fig. 5. Though the trends are similar, the absolute values are different, possibly due to the different crystal orientation or lattice parameter, i.e. crystallinity, stress and orientation effect band gap values [6,17,18]. The trend follows [19].

$$E = E_g(\text{bulk}) + \frac{\hbar^2\pi^2}{2}\left(\frac{1}{m_e^*} + \frac{1}{m_h^*}\right)\frac{1}{r^2} \tag{4}$$

or

$$E = E_g(\text{bulk}) + \frac{\hbar^2\pi^2}{2\mu^* r^2} \tag{5}$$

where $E_g(\text{bulk})$ is the band gap of SnS in bulk, 'm_e^*' and 'm_h^*' are the effective mass of electron and holes, respectively.

This result is consistent with properties induced by quantum confinement of charge carriers [19]; confirming that SnS grains of 11–25 nm are in the nano-regime.

It would appear that the SnS grains with size greater than 25 nm would have a band gap similar to the bulk. Curve fits for data points in Fig. 5 gives $E_g(\text{bulk})$ for glass and ITO as 1.707 and 1.65 eV respectively. We believe that the difference in the value is a result of the different orientations in which the SnS film exists on glass and ITO substrates. The above data also allows us to explore variation in effective mass in different directions of SnS crystal. Using our experimental data, we can only comment on the reduced effective mass (μ^*). The reduced effective mass from curve fitting is $0.68m_o$ and $0.65m_o$ for samples on glass and ITO substrates, respectively, where m_o is the rest mass of a free electron.

It can be seen from Fig. 6, the band gap of SnS thin films increases with increasing lattice parameter 'a' for both cases of films, grown on glass and ITO substrates. As explained by Eq. (2), an increase in lattice parameter is indicative of a stress acting along 'a'. Fig. 6 shows that the stress is greater in films fabricated on ITO substrates [20]. The difference in strain ($\text{strain}_{\text{glass}} < \text{strain}_{\text{ITO}}$) stems from the difference in orientation between the films on different substrates. The data points from both the substrates do not lie on a single line. This is indicative of the fact that SnS band gap depends on the lattice parameter and a second variable, possibly the grain size (from Fig. 5). Experimentally, the different substrate used and variation in film thickness controlled the two "variables". Theoretically, however, we can only study the variation of band gap as a function of lattice parameters (or in other words unit cell volume). In the next section we investigate the results of Fig. 6 using theoretical calculations.

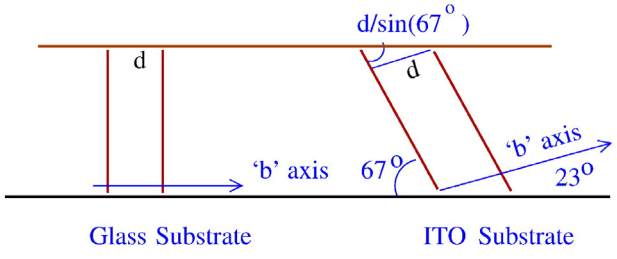

Fig. 3. Schematics shows orientation of our SnS samples on the two substrates.

4. Band structure calculation

The band structure of SnS has been theoretically evaluated quite extensively [7,13,14,21,11]. We have performed ab initio calculations of the SnS electronic band structure in the framework of the density functional theory (DFT) as implemented in the WIEN2k software [22], adopting the Engel-Vosko approximation for the exchange-correlation potential. We analysed the energetic behaviour of the compound with the inclusion of the spin orbit interaction. We have used the lattice parameters obtained experimentally for the various SnS films with 4 Sn and 4 S atoms (8 atoms) per unit cell, forming two parallel zigzag chains for the calculations. To achieve total convergence in the self-consistent calculations, we used RKMAX equal to 7, and a converged sampling of 194 k-point in the first Brillouin Zone (BZ).

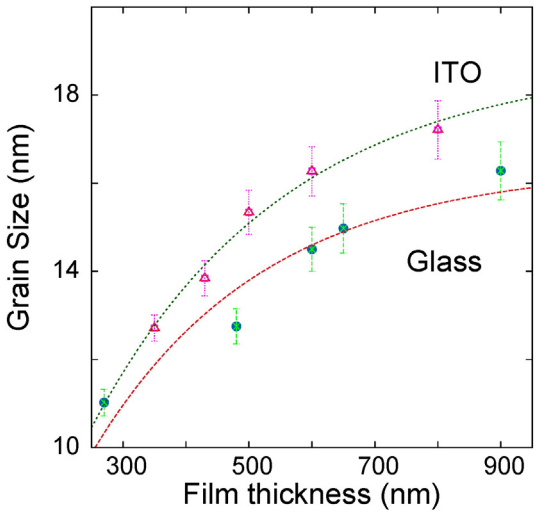

Fig. 4. Variation in grain size with film thickness for SnS films grown on glass and ITO substrates.

Table 1A
List of lattice constants, average grain size (GS) and energy band-gaps of SnS films for different film thicknesses grown on glass substrates.

Thickness (nm)	a (nm)	b (nm)	c (nm)	GS (nm)	E_g (eV)
270	0.450	1.141	0.417	11.02	2.02
480	0.427	1.140	0.417	12.75	1.95
600	0.407	1.138	0.417	14.50	1.88
650	0.407	1.139	0.417	14.97	1.87
900	0.408	1.137	0.417	16.28	1.85

4.1. Structure of SnS for various lattice parameters

As stated in the preceding section, we had deposited SnS films on ITO and glass substrates. We experimentally determined the lattice parameters for these samples. Using these lattice parameters, we computed the band structure of SnS thin films (Fig. 7). Since the lattice parameter 'b' showed insignificant variation with thickness in samples grown on glass and ITO substrates, we concluded that 'b' lattice parameter does not contribute to the variation in the band gap. Its contribution is only along the Γ→Y direction of the BZ [7] where the "energy difference" (difference in valence band maximum and conduction band minimum) is too large to be considered as energy band gap associated with SnS.

However, many other valence band maximas and conduction band minimas are visible in the Γ→X and Γ→Z. In fact, in one of the author's previous studies [11], it was demonstrated that SnS and their related IV-VI orthorhombic compounds exhibit several direct and indirect gaps which are close in energy and competing to form the band gap. This makes it difficult to precisely determine whether the band gap is direct or indirect (confirmed by experimental works also [24,25,10]). Careful analysis of Fig. 7 shows two comparable energy differences each contributing to the energy band gap of SnS films on glass and ITO substrates respectively. The calculated band gaps are smaller than the experimental ones due to the well known underestimation that DFT provides. This, however, can be overcome by including the many-body electron-electron interaction, within the GW Hedin and Lundskvit [26,27] formalism. We had previously calculated this correction for the semiconductor SnS [11], obtaining a constant potential value of 0.38 eV giving a good agreement with the experimental values. We have added this correction to all the calculated band gaps.

In SnS films grown on ITO substrates, the smallest "energy difference" is the quasi-direct energy gap formed between the V1 relative maximum in the valence band, and the minimum of the conduction band at C1, located at about 1/4 from the Z point of the Γ→Z direction of the BZ. The variation in this band gap with the normalized lattice's unit cell volume is shown in Fig. 8. For obtaining the normalized lattice's unit cell volume, the stressed lattice's unit volume is divided by the volume listed in the given ASTM Card (henceforth lattice's unit cell volume would imply normalized lattice's unit cell volume).

The films on glass substrates show two important energy gaps, they are both quasi-direct, one along the Γ→Z direction of the BZ that occurs at 1/4 from Z point (V1 to C1) and second along the Γ→X direction of the BZ (V2 to C2). The variation of band gap with lattice's unit cell volume is shown in Fig. (8). In Fig. (8), we have included the experimental data (filled and unfilled circles with trend lines are for SnS films on glass and ITO substrates respectively) along with the theoretically calculated values. Considering that the experimental method matched well with the Γ→Z contributions, the band gaps calculated along the Γ→X has not been shown in Fig. 8 for brevity. Also, the present calculations and inference that the direct band-gap is along the Γ→Z is in agreement with earlier works [14]. Also, the order of band-gap is also in agreement, with Georgios et al. [14] calculations for bulk giving the band-gap to be 1.65 eV.

Considering that the variation in lattice parameters would result in residual stress effects that would manifest as pressure, we expect changes in the conduction band, valence band shapes and band gaps [14,11]. Georgies et al. [14], Makinistian et al. [11] and Parenteau et al. [23] works show that the band gap of SnS is directly proportional to the unit cell's volume, with band gap approaching small values as volume decreases. Fig. 8 also shows the results of our calculations for samples grown on ITO and glass respectively for different thicknesses. The linearity is in confirmation of results in the literature and experimental results highlighted in Figs. (6) and (8). The theoretical work, hence matches and substantiates the experimental results. However, the theoretical calculations of band structure do not take into account

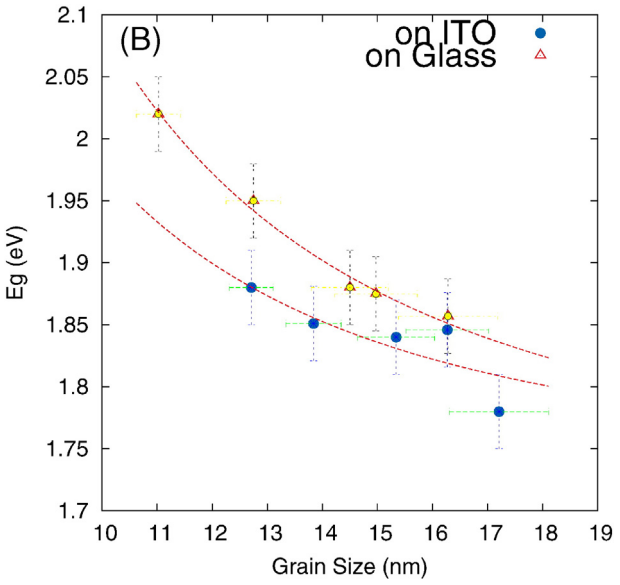

Fig. 5. Variation of the band gap with grain size.

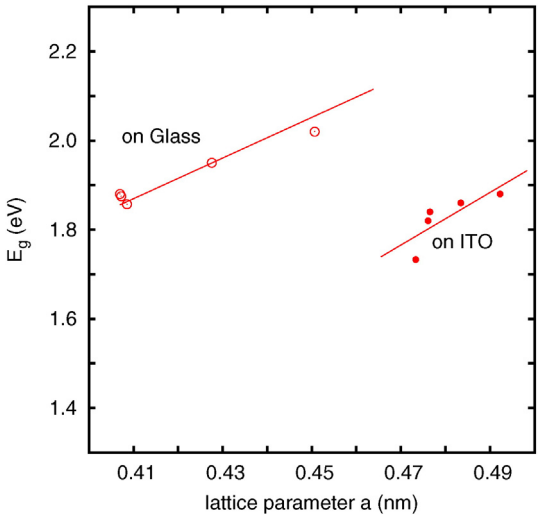

Fig. 6. A linear variation is found in SnS band gap with increasing lattice parameter 'a'.

Table 1B
List of lattice constants, average grain size (GS) and energy band-gaps of SnS films for different film thicknesses grown on ITO substrates.

Thickness (nm)	a (nm)	b (nm)	c (nm)	GS (nm)	E_g (eV)
330	0.492	1.135	0.376	12.71	1.88
430	0.483	1.133	0.378	13.84	1.85
400	0.476	1.134	0.378	15.34	1.84
610	0.476	1.130	0.369	16.27	1.84
800	0.473	1.130	0.382	17.21	1.78

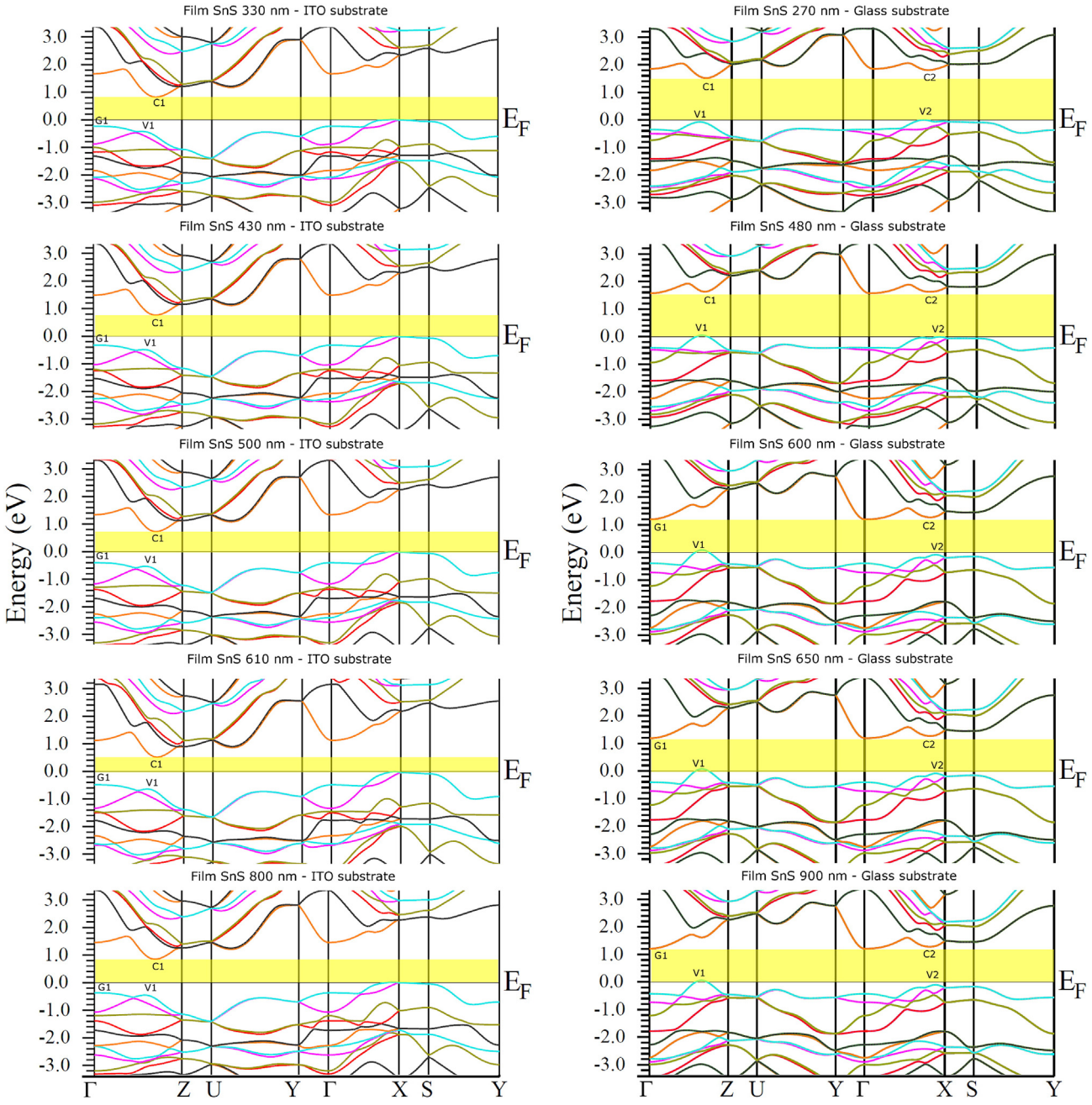

Fig. 7. Results of electronic band structure calculations for SnS thin films on ITO and glass substrates. A constant GW potential of 0.38 eV was added to the band gaps values (not shown in these plots but it is included in all the band gap values considered in the rest of the paper).

grain boundary and hence we are not in a position to comment on the variation of band gap with grain size. As stated in our section on experimental results, the band gap depends on both the grain size and lattice's unit cell volume (via lattice parameter). To this extent, we believe that the two variables are acting independently of each other and are hence separable. Eq. (5) should then be written as.

$$E(r,V) = \left(\frac{V}{V_o}\right) E_g(\text{bulk}) + \frac{\hbar^2 \pi^2 V}{2\mu^* V_o}\left(\frac{1}{r^2}\right) \tag{6}$$

Fig. (9) shows a plot of our experimental data along with data collected from various literature [15,28–36] on SnS thin films. It is seen that the data points arrange themselves along two families of graphs, namely on $V/V_o \approx 0.975$ and 0.995 for various grain sizes (i.e. displaced along the V/V_o axis, which is a measure of the variation in lattice parameters). Five data points (indicated with downward pointing triangles) lie on the curve for $V/V_o \approx 0.975$. Our experimental data for films grown on glass fall on this curve. A large volume of data exists for $V/V_o \approx 0.995 - 1$. Again, if we consider Eq. (5) to be valid, then a family of curves should not have existed. If forced to curve fit, fitting should return identical values of $E_g(\text{bulk})$ and $\frac{\hbar^2\pi^2}{2\mu}$. This is not the case. A look into the derivation of Brus [19] Eq. (5) would show that it considers the electron's Coulombic interactions only. This interaction becomes prominent only when the electrons are confined in grains whose dimensions are on the nano-scale. In large crystals, these interactions are neglected since the electrons are far apart and their interactions are only with the lattice potential whose periodicity is related to the lattice parameter. The curvature of the band structures, formed due to

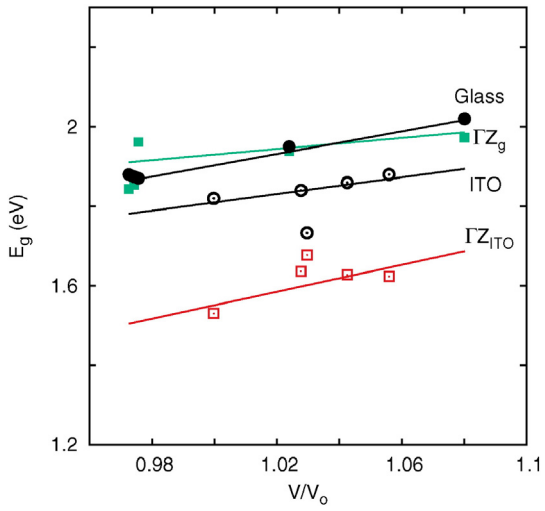

Fig. 8. Plots show the band gaps of SnS films as a function of the lattice's unit cell volume. Full squares (trend marked by a green solid line) represent the quasi-direct band gaps in the 'c' axis direction (Γ→Z direction in the BZ) for SnS films on glass substrates. The unfilled squares (trend marked by a red solid line) represent the quasi-direct band gaps in the 'c' axis direction (Γ→Z direction in the BZ) for SnS films on ITO substrates. For comparing, full circles and unfilled circles with black solid lines are given which represent the experimental band gaps of SnS films on glass and ITO substrates respectively. (For interpretation of the references to color in this figure legend, the reader is referred to the web version of this article.)

the electron lattice potential interaction, is related to the magnitude of the effective mass. Our results suggest, that even at the nano-scale, the electron lattice potential interaction cannot be neglected and has to be considered along with the electron-electron interaction potential. Results emerging from Fig. (9) suggest that resulting Schrodinger equation is solvable by separable variable method leading to an expression as given in Eq. (6).

Taking into account the lattice parameter, we have reduced effective mass for ($V/V_o \approx$) 0.975 and 0.995 as $0.247m_o$ and $0.279m_o$, respectively. This is nearer to the theoretical calculations in literature [5,13,14] and also confirmed by our own theoretical calculations. The data points on the two sets of curves of Fig. (9) are from various sources and include those on glass and ITO substrates. Hence, the trend now is fully explained by grain size and lattice parameter.

5. Conclusions

Tin sulphide nano-crystalline thin films were fabricated on glass and ITO substrates by thermal evaporation method. The crystal structure orientation was different for the two different substrates. Residual stress due to these orientations leads to variation in unit cell lattice parameters. The lattice parameters were found to vary with film thickness. The nano-crystalline grain size was also found to be thickness dependent. While the band-gap of the films for same lattice constants and varying grain size showed the classical quantum confinement relation, samples with varying lattice constant did not fall on the trend. Theoretical electronic structure calculations for different lattice constants were made and it showed that the experimental data followed the calculated trend. This confirmed our hypothesis that the band gap has a two variable dependency. The results also allowed us to show the dependency of effective mass (reduced) on the lattice unit volume. We believe the results are of significance in material science where material characteristics can be manipulated as per requirement.

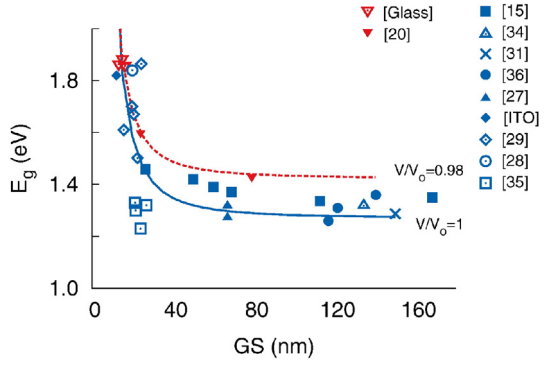

Fig. 9. The band gap is plotted as a function of normalized lattice volume and grain size (GS). The points arrange in two curves, namely $V/V_o \approx 0.98$ and $V/V_o \approx 1$ (data points indicated with red triangles and blue colored shapes respectively). The source of references are indicated. (For interpretation of the references to color in this figure legend, the reader is referred to the web version of this article.)

Acknowledgement

Discussions with Sukanta Dutta, Department of Physics, S.G.T.B. Khalsa College are gratefully acknowledged. One of the authors (YG) would like to acknowledge DST (India) for the fellowship (Fellowship No. IF131164) awarded under its Inspire Scheme. The authors (AAN, MVW and EAA), acknowledge the financial support from the Universidad Nacional de Entre Ríos (UNER), Argentina. EAA also acknowledge finantial support from the Consejo Nacional de Investigaciones Científicas y Técnicas (CONICET), Argentina, through grant (PIP 11220150100124CO).

References

[1] C. Gao, H. Shen, Z. Shen, Mater. Lett. 65 (2011) 1413.
[2] G.H. Yue, D.L. Peng, P.X. Yan, L.S. Wang, W. Wang, X.H. Luo, J. Alloys Compd. 468 (2009) 254.
[3] O.E. Ogah, K. Ramakrishna Reddy, G. Zoppi, I. Forbes, R.W. Miles, Thin Solid Films 519 (2011) 7425.
[4] M. Leach, K.T. Ramakrishna Reddy, M.V. Reddy, J.K. Tan, D.Y. Jang, R.W. Miles, Energy Procedia 15 (2012) 371.
[5] W. Albers, C. Haas, H.J. Vink, J.D. Wasscher, J. Appl. Phys. 2 (1961) 2220.
[6] P. Sinsermsuksakul, J. Heo, W. Noh, A.S. Hock, R.G. Gordon, Adv. Energy Mater. 1 (2011) 1116.
[7] L. Makinistian, E.A. Albanesi, Phys. Status Solidi B 246 (2009) 183.
[8] S.A. Bashkirova, V.F. Gremenoka, V.A. Ivanova, V.V. Shevtsovaa, P.P. Gladyshev, Thin Solid Films 585 (2015) 40.
[9] A. Jakhar, A. Jamdagni, A. Bakshi, T. Verma, V. Shukla, P. Jain, N. Sinha, P. Arun, Solid State Commun. 168 (2013) 31.
[10] P. Jain, P. Arun, Thin Solid Films 548 (2013) 241.
[11] L. Makinistian, E.A. Albanesi, Comput. Mater. Sci. 50 (2011) 2872.
[12] E.D. Cullity, S.R. Stock, Elements of X-Ray Diffraction, third ed. Prentice-Hall Inc., NJ, 2001.
[13] J. Vidal, S. Lany, M. d'Avezac, A. Zunger, A. Zakutayev, J. Franeis, J. Tate, Appl. Phys. Lett. 100 (2012) 032104.
[14] G.A. Tritsaris, B.D. Malone, E. Kaxiras, J. Appl. Phys. 113 (2013) 233507.
[15] M. Devika, N.K. Reddy, K. Ramesh, H.R. Sumana, K.R. Gunasekhar, E.S.R. Gopal, K.T. Ramakrishna Reddy, Semicond. Sci. Technol. 21 (2006) 1495.
[16] J. Tauc, Mater. Res. Bull. 5 (1970) 721.
[17] M. Ristov, G. Sinadinovski, J. Grozdanov, M. Mitreski, Thin Solid Films 173 (1989) 53.
[18] P. Tyagi, A.G. Vedeshwar, Phys. Rev. B 63 (2001) 245315.
[19] L.E. Brus, J. Chem. Phys. 80 (1984) 094403.
[20] B. Ghosh, M. Das, P. Banerjee, S. Das, Semicond. Sci. Technol. 23 (2008) 125013.
[21] L. Ehm, K. Knorr, P. Dera, A. Krimmel, P. Bouvier, M. Mezouar, J. Phys. Condens. Matter 16 (2004) 3545.
[22] P. Blaha, K. Schwarz, J. Luitz, Viena University of Technology, 2001. Improved and updated version of the WIEN code, published by P. Blaha, K. Schwarz, P. Sorantin, S.B. Rickey, Comput. Phys. Commun. 59 (1990) 399.
[23] M. Parenteau, C. Carlone, Phys. Rev. B 41 (1990) 5227.
[24] M. Calixtro-Rodriguez, H. Martinez, A. Sanchez-Juarez, J. Campos-Alvarez, A. Tiburcio-Silver, M.E. Calixto, Thin Solid Films 517 (2009) 2497.
[25] X. Gou, J. Chen, P. Shen, Mater. Chem. Phys. 93 (2005) 557.
[26] L. Hedin, S. Lundqvist, Solid State Phys. 23 (1970) 1.
[27] L. Hedin, Phys. Rev. 139 (1965) A796.
[28] M. Devika, K.T. Ramakrishna, N.K. Reddy, K. Ramesh, R. Ganesan, E.S.R. Gopal, K.R. Gunasekhar, J. Appl. Phys. 100 (2006) 023518.
[29] E. Turan, M. Kul, A.S. Abyek, M. Zor, J. Phys. D. Appl. Phys. 42 (2009) 245408.
[30] Y. Aziyan-Kalandaragh, A. Khodayari, Z. Zeng, C.S. Garoufalis, S. Baskoutas, L.C. Gontard, J. Nanopart. Res. 15 (2013) 1388.
[31] T.H. Patel, Open Surf. Sci. J. 4 (2012) 6.
[32] A. Gomez, H. Martinez, M. Calixto-Rodriguez, D. Avellaneda, P.G. Reyes, O. Flores, J. Mater. Sci. Eng. B 3 (2013) 352.

[33] T.H. Sajessh, A.R. Warrier, C.S. Kartha, K.P. Vijayakumar, Thin Solid Films 518 (2010) 4370.
[34] M. Devika, N.K. Reddy, K. Ramesh, K.R. Gunasekhar, E.S.R. Gopal, K.T.R. Reddy, Semicond. Sci. Technol. 21 (2006) 1125.
[35] S. Chen, Y. Chen, Y. He, G. Chen, Mater. Lett. 61 (2007) 1408.
[36] M. Devika, N.K. Reddy, D.S. Reddy, S.V. Reddy, K. Ramesh, E.S.R. Gopal, K.R. Gunasekhar, V. Ganesan, Y.B. Hahn, J. Phys. Condens. Matter 19 (2007) 306003.